Transient State Modeling of Asynchronous Generator with Skin-Effect

Dr.-Ing. O. I. Okoro

Department of Electrical Engineering
University of Nigeria, Nsukka
Enugu State, Nigeria.
Email: ogbonnayaokoro@hotmail.com

ABSTRACT

When asynchronous machines are used as wind energy turbine generators, problems arise if the actual machine behavior under transient conditions is not properly determined prior to loadability. This paper presents the improved modeling of an asynchronous generator by including skin-effect, which the conventional model excludes. The results of the conventional model are presented, and a comparison is made with the proposed skin-effect model. The error in the former, underscores the need for the proposed skin-effect model, especially in wind energy plants where variation in load and rotor speed are common features.

(Key words: asynchronous machine, wind energy, turbine generators, skin-effect, transient state)

INTRODUCTION

Developing countries have devoted much attention to rural electrification projects. This is understandable because the light, refrigeration, mechanization, and communication that even a small amount of electricity can provide, produces a high return in the enhancement of the health, social welfare, and overall productivity of the rural populace. Unfortunately, the pace of rural electrification is usually very sluggish in execution, to the dislike of the beneficiaries. It is also very capital intensive and has very unfavorable short-term economics [1].

However, the use of centrally located power plants and grid extension systems for rural electrification is being challenged today due to the advent of smaller, modular, and efficient generating technologies, such as wind power, micro-hydro, and photovoltaics [2].

In order to embrace these new technologies, a look at the dynamic performance of the wind turbine generators, which are usually totally enclosed fan cooled (TEFC) induction machines, becomes highly imperative. In the past, induction generators have been rejected for power generation because of the attention given to synchronous generators [3]. However, it has been noted that the induction generator has advantages over the classical synchronous generator, for wind turbine applications [4]. These advantages include: elimination of start-up problems, and a much reduced distortion factor. In this paper, the transient state modeling of a 7.5KW Squirrel-cage induction generator is presented. The conventional model development is first presented followed by the skin-effect model. The method of solution and the simulation results are thereafter discussed.

CONVENTIONAL MACHINE MODEL

In the development of the conventional machine model, the following assumptions are made:

1. The stator voltages are balanced.
2. The machine is symmetrical with linear magnetic circuit.
3. Skin-effect and saturation effect are neglected.
4. Harmonic content of the mmf wave is neglected.

The most commonly used transient state conventional model is the d-q axis frames of reference representation, as reported by Krause and Thomas [5]. The d-q axis model of the motor provides a convenient way of modeling the machine and is most suitable for numerical

solution. This is preferable to the space-vector machine model, which describes the machine in terms of complex variable [6]. Figure 1 shows the direct and quadrature representation of the squirrel-cage induction machine in schematic form.

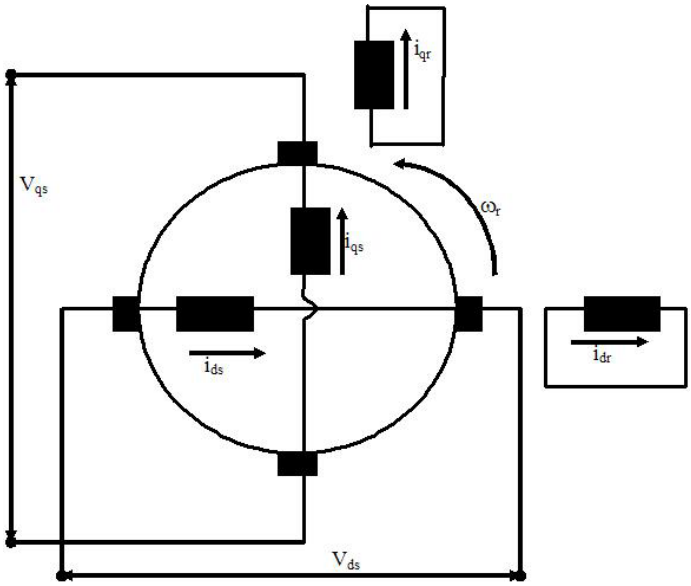

Figure 1: Schematic form of Squirrel-Cage Induction Machine Showing d-q axis.

The d-q axis stator and rotor voltages for an ideal symmetrical induction machine in arbitrary reference frame are expressed as in [5].

$$V_{ds} = R_s i_{ds} + \frac{d}{dt}\lambda_{ds} - \omega\lambda_{qs} \quad \text{..... (1)}$$

$$V_{qs} = R_s i_{qs} + \frac{d}{dt}\lambda_{qs} + \omega\lambda_{ds} \quad \text{..... (2)}$$

$$V'_{dr} = R'_r i_{dr} + \frac{d}{dt}\lambda_{dr} - (\omega - \omega_r)\lambda_{qr} \quad \text{..... (3)}$$

$$V'_{qr} = R'_r i_{qr} + \frac{d}{dt}\lambda_{qr} - (\omega - \omega_r)\lambda_{dr} \quad \text{..... (4)}$$

Equations (1-4) can be expressed in state variable form with flux linkages as state variables [7].

$$\dot{\lambda}_{ds} = V_{ds} - i_{ds}R_s + \omega\lambda_{qs} \quad \text{..... (5)}$$

$$\dot{\lambda}_{qs} = V_{qs} - R_s i_{qs} - \omega\lambda_{ds} \quad \text{..... (6)}$$

$$\dot{\lambda}_{dr} = -R'_r i_{dr} + (\omega - \omega_r)\lambda_{qr} \quad \text{..... (7)}$$

$$\dot{\lambda}_{qr} = -R'_r i_{qr} - (\omega - \omega_r)\lambda_{dr} \quad \text{..... (8)}$$

and,

$$\begin{bmatrix} i_{ds} \\ i_{qs} \\ i_{dr} \\ i_{qr} \end{bmatrix} = K_o \begin{bmatrix} \frac{L_r}{L_m} & 0 & -1 & 0 \\ 0 & \frac{L_r}{L_m} & 0 & -1 \\ -1 & 0 & \frac{L_s}{L_m} & 0 \\ 0 & -1 & 0 & \frac{L_s}{L_m} \end{bmatrix} \begin{bmatrix} \lambda_{ds} \\ \lambda_{qs} \\ \lambda_{dr} \\ \lambda_{qr} \end{bmatrix} \quad \text{(9)}$$

In these equations: λ_{ds} ,λ_{qs} , λ_{dr}, and $\lambda_{qr,}$ are the linkage fluxes along the d and q axes of the stator and rotor. Ls and Lr are the inductances of the stator and rotor d-q equivalent windings. Rs and Rr are the resistances of the stator and rotor windings. Lm is the mutual inductance between the stator and rotor windings. And, δ is the dispersion coefficient of the machine, which is expressed as:

$$\delta = 1 - \frac{L_m^{\ 2}}{L_r L_s} \quad \text{..... (10)}$$

where,

$$K_o = \frac{1-\delta}{\delta L_m} \quad \text{..... (11a)}$$

$$L_s = L_{ls} + L_m \quad \text{..... (11b)}$$

$$L_r = L'_{lr} + L_m \quad \text{..... (11c)}$$

The voltages V_{ds} and V_{qs} represent the applied stator voltages in the orthogonal coordinate system, and are related algebraically to these voltages. The voltages V_{dr} and V_{qr} as well as other rotor variables are referred to the stator by the effective stator/rotor turns ratio. Since the test machine is a squirrel-cage type, the rotor windings are shorted; thus the rotor voltages are identically equal to zero. The equations of transformation relating the d-q-o stator and rotor voltages to the actual applied voltages are given in [8] as:

$$\begin{bmatrix} i_{qs} \\ i_{ds} \\ i_{0} \end{bmatrix} = [C] \begin{bmatrix} i_{as} \\ i_{bs} \\ i_{cs} \end{bmatrix} \quad \text{..... (12)}$$

$$\begin{bmatrix} i_{as} \\ i_{bs} \\ i_{cs} \end{bmatrix} = [C]^{-1} \begin{bmatrix} i_{qs} \\ i_{ds} \\ i_{0} \end{bmatrix} \quad \text{..... (13)}$$

where,

$$[\mathbf{C}] = \frac{2}{3} \begin{bmatrix} \cos\theta & \cos\left(\theta - \frac{2\pi}{3}\right) & \cos\left(\theta - \frac{4\pi}{3}\right) \\ \sin\theta & \sin\left(\theta - \frac{2\pi}{3}\right) & \sin\left(\theta - \frac{4\pi}{3}\right) \\ \frac{1}{2} & \frac{1}{2} & \frac{1}{2} \end{bmatrix} \quad \text{(14)}$$

$$[\mathbf{C}]^{-1} = \begin{bmatrix} \cos\theta & \sin\theta & 1 \\ \cos\left(\theta - \frac{2\pi}{3}\right) & \sin\left(\theta - \frac{2\pi}{3}\right) & 1 \\ \cos\left(\theta - \frac{4\pi}{3}\right) & \sin\left(\theta - \frac{4\pi}{3}\right) & 1 \end{bmatrix} \quad \text{(15)}$$

In the analysis of induction machines, it is always advisable to transform equations (5-8) to d-q axis fixed either on the stator [9], or the rotor [10], or rotating in synchronism with the supply voltages [11]. In [9], equations (5-8) are modified by setting ω=0 and in [10], $\omega=\omega_r$, while in [11] $\omega=\omega_e$. It is important to note that the choice of reference frame will affect the waveforms of all d-q variables, and also the simulation speed as well as the accuracy of the results. For analyses involving saturation and deep bar effect, a reference frame fixed to the rotor is recommended [12].

MECHANICAL MODEL

The mechanical model of the induction machine can be expressed as two first-order systems of differential equations.

$$\frac{d\omega_r}{dt} = \frac{1}{J_m}\left(T_e + T_m\right) \quad \text{..... (16)}$$

$$\frac{d\theta_r}{dt} = \omega_r \quad \text{..... (17)}$$

$$\omega_r = \omega_m P \quad \text{..... (18)}$$

The electromagnetic torque, Te is given by [13] as:

$$T_e = 1.5P\left(\lambda_{ds} i_{qs} - \lambda_{qs} i_{ds}\right) \quad \text{..... (19)}$$

Where,

ω_r = Angular velocity of the rotor,

ω_m = Mechanical rotor speed,

P = Number of pole pairs

T_e = Electromagnetic torque,

T_m = Load torque,

θ_r = Rotor angular position,

J_m = Combined rotor and load inertia.

Since the Asynchronous machine is operating in generating mode, the sign of the mechanical torque is negative. Figure 2 shows the block diagram representation for modeling both the electrical and mechanical models of the machine, in an arbitrary reference frame.

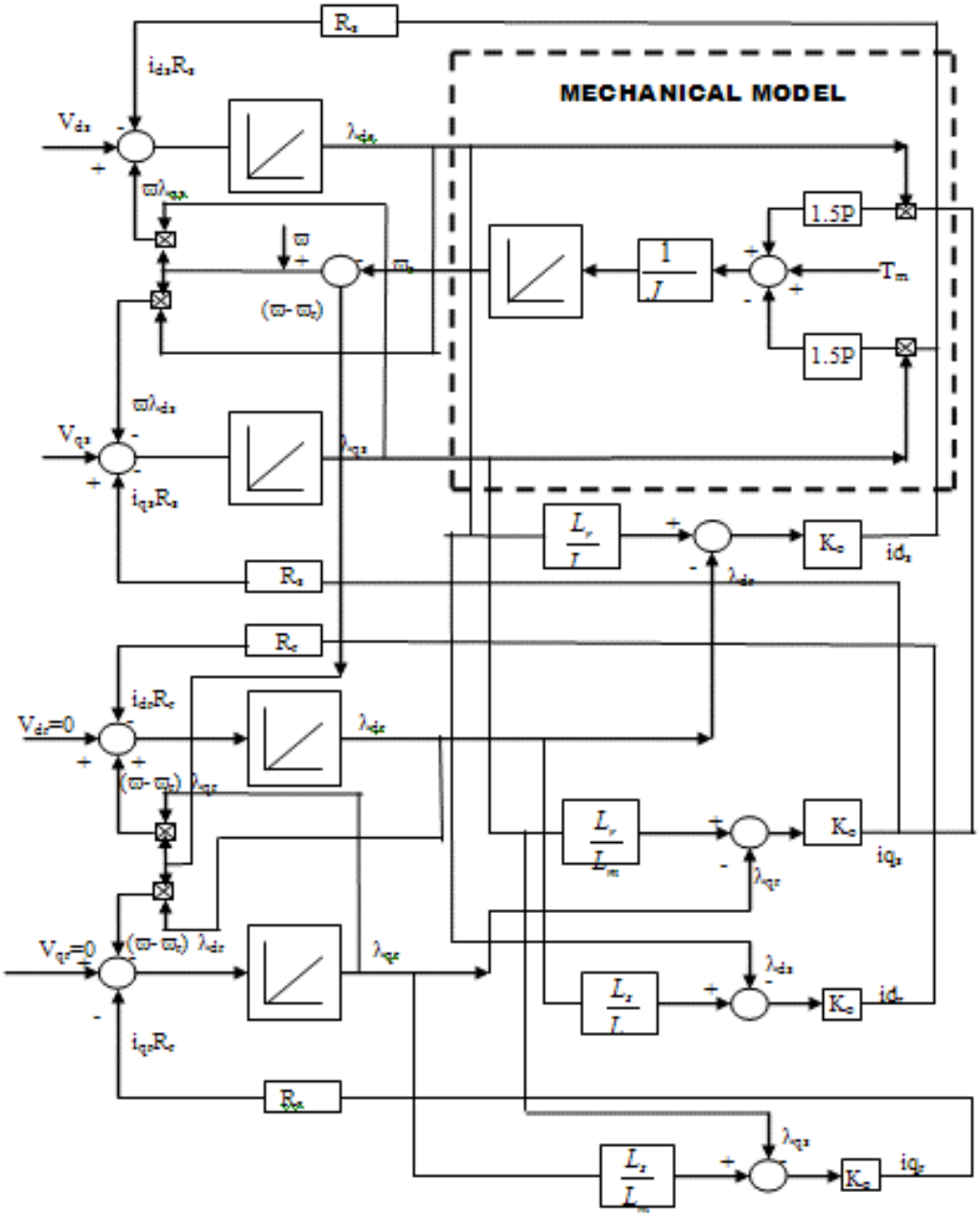

Figure 2: Block diagram representation of Asynchronous generator.

SKIN-EFFECT MODEL

When bar conductors are contained in slots the leakage flux causes the current to crowd towards the top of the bar adjacent to the air gap. Because this effect is a function of frequency, the effective resistance and reactance of a rotor bar will change during speed variations, especially during the run-up period.

The aftermath of this current migration is to reduce the apparent inductance of the rotor conductors, and to increase their resistance. The magnitude of these changes is very much dependent on the design of the rotor bars. For a rectangular rotor-bar, two approaches can be used to incorporate this effect. One is by the use of numerical expression according to Alger [14]. The second represents the eddy currents by additional circuit equations in the form of a ladder networks as reported by [8]. For the simplest case of a rectangular bar such as the one shown in figure 3, the Alger method is generally recognized to yield acceptable results, for the majority of problems encountered in electrical machine dynamics [12].

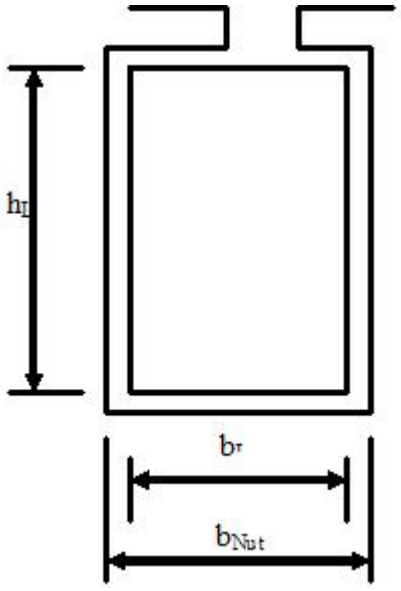

Figure 3: Rectangular Rotor Bar.

The Alger expressions for the rectangular-rotor bar resistance and reactance are given as in [14].

$$K_r = \xi\left[\frac{\sinh 2\xi + \sin 2\xi}{\cosh 2\xi - \cos 2\xi}\right] \quad \text{(20)}$$

$$K_e = \frac{3}{2\xi}\left[\frac{\sinh 2\xi - \sin 2\xi}{\cosh 2\xi - \cos 2\xi}\right] \quad \text{(21)}$$

In these equations, ξ is defined as:

$$\xi = 2\pi h_L\left(\frac{kf}{\rho} * 10^{-7}\right)^{\frac{1}{2}} \quad \text{(22)}$$

$$R_2 = K_r R_{20} \quad \text{(23)}$$

$$X_2 = K_e X_{20} \quad \text{(24)}$$

$$k = \frac{b_L}{b_{Nut}} \quad \text{(25)}$$

R_{20} and X_{20} in the above equations represent the dc value of the resistance, and the dc value of the reactance.

By incorporating equations (23) and (24) into the conventional model, the values of the rotor resistance, and the rotor inductance, can be made to vary with frequency at each integration step.

METHOD OF SOLUTION AND RESULTS

The test machine used in this study was a KATT VDE 0530, class F insulation, Squirrel-cage induction generator as shown in Figure 4.

Figure 5 shows the rotor part of the test machine. In order to determine the test machine parameters, no-load, load, D.C. measurement, blocked rotor, and retardation tests were carried out on this machine.

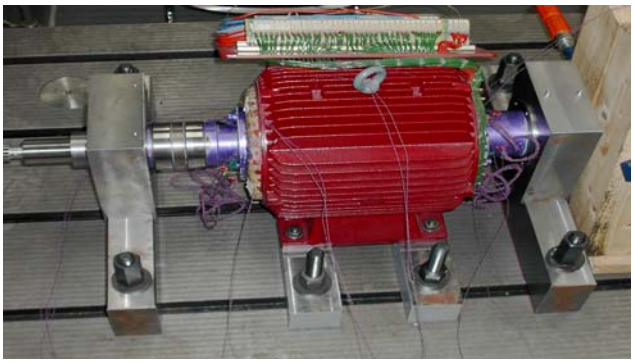

Figure 4: The 7.5KW Squirrel-Cage Induction Generator.

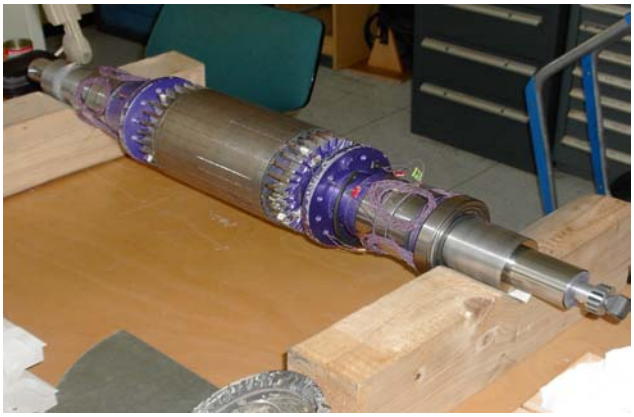

Figure 5: Rotor Part of the Test Machine.

The no-load test was carried out at the rated frequency and with the balanced polyphase voltages applied to the stator terminals. Readings for current, voltage, electrical power and speed, were taken after the motor ran for the period of time necessary for the bearings to be properly lubricated.

Blocked-rotor tests and tests with the injection of D.C. current in the stator windings were made at standstill. The retardation test was carried out at no-load, with and without additional standard mass. The load test was carried out with constant load and frequency at a sinusoidal stator windings voltage. Table 1 shows the test machine parameters obtained through this process. The measured rotor-bar parameters are also included in the table.

In order to verify the validity of the developed models, a MATLAB m-file [15] was developed.

The non-linear system of differential equations governing the transient behavior of the machine, were first solved for the conventional model using the Fourth-order Runge-Kutta method. In this case, the values of the rotor resistance and inductance are constant. The second case considers the skin-effect on the rotor bar by making use of the Alger numerical expressions to vary the values of the rotor resistance and reactance at each integration step.

Table 1: Test Machine Data.

Output Power	7.5KW
Rated voltage	340V
Winding connection	Delta
Number of Poles	4
Rated speed	1400rpm
Rated frequency	50Hz
Stator resistance	2.52195ohm
Stator leakage reactance	1.95145ohm
Rotor resistance	0.976292ohm
Rotor leakage reactance	2.99451ohm
Magnetizing reactance	55.3431ohm
Mechanical shaft torque	51.2636N.m
Estimated rotor inertia moment	0.117393Kgm^2
Rated current	19.2A
Moment of inertia of the D.C. motor	0.10958Kgm^2
Shaft stiffness constant	14320Nm/rad
Insulation thickness	0.3mm
Height of rotor bar	13.2mm
Width of rotor bar	4.4mm
Bar length	239mm
Conductivity of rotor bar	$56Sm/mm^2$
Permeability of free space	$4\pi*10^{-7}H/m$

Figure 6 shows the computed transient behavior of the induction generator at run-up condition using the conventional model. Figure 7 shows that of the skin-effect model.

Figure 8 and figure 9 show the computed stator phase currents for the conventional model and the skin-effect model, respectively.

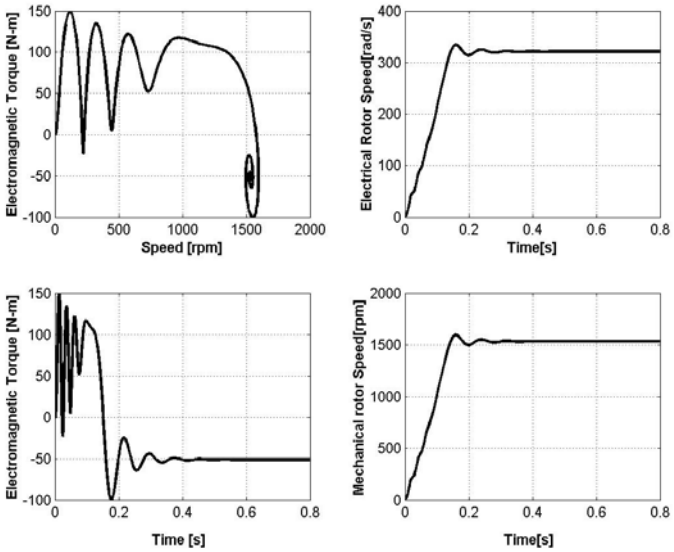

Figure 6: Machine Run-Up Characteristics: Conventional Model.

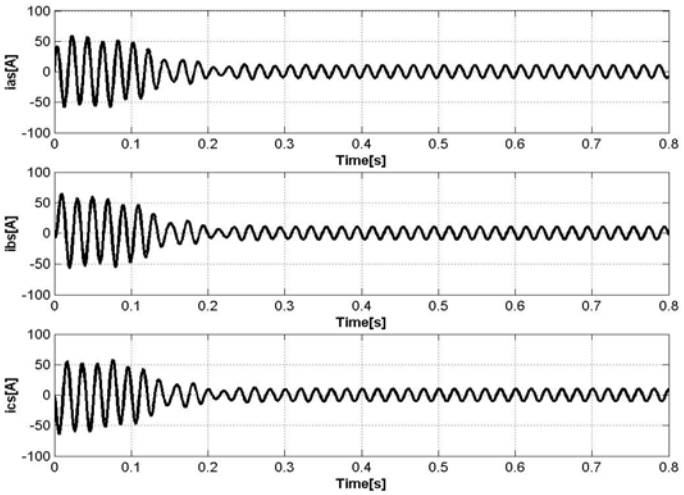

Figure 8: Stator Phase Currents: Conventional Model.

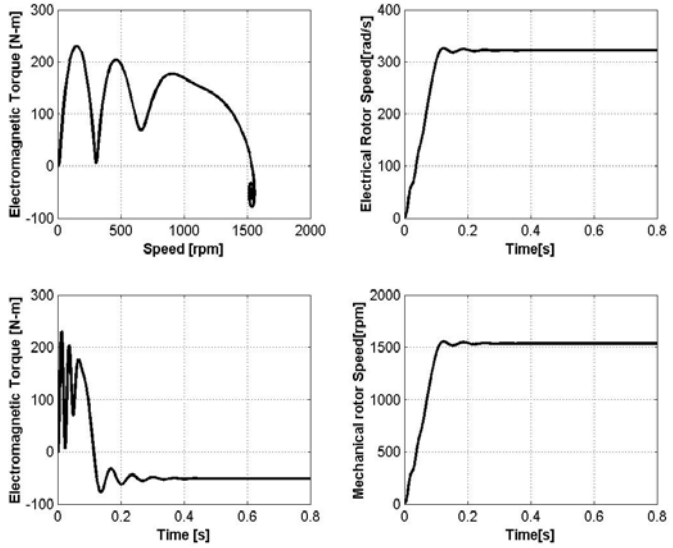

Figure 7: Machine Run-Up Characteristics: Skin-Effect Model.

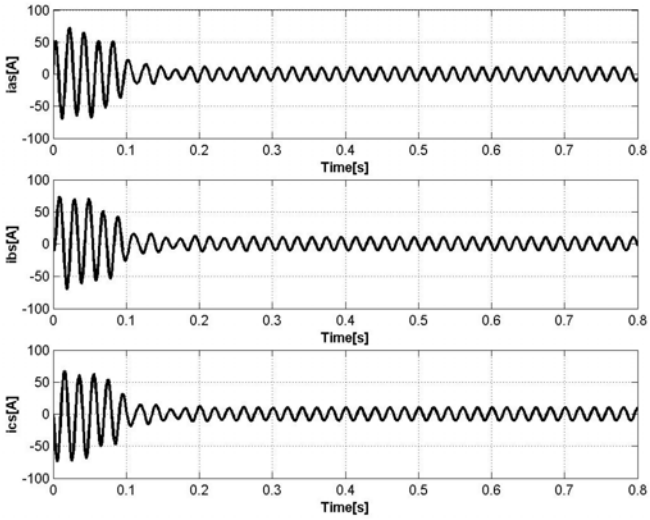

Figure 9: Stator Phase Currents: Skin-Effect Model.

In order to visualise the difference in the two models, comparison is made between the conventional model mechanical speed, Electromagnetic torque, and stator phase currents, with that of the skin-effect model. Figure 10, Figure 11, Figure 12 and Figure 13 show these comparisons.

CONCLUSIONS

This paper presents two models for Squirrel-cage induction generator for transient operation. Their parameters are readily obtained from the No-load, Blocked rotor, D.C. measurement, and retardation tests.

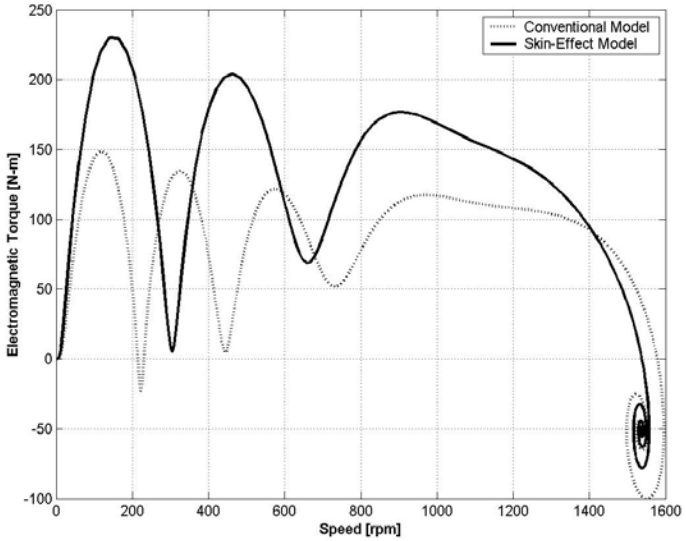

Figure 10: Electromagnetic Torque-Speed Plot for the two Models.

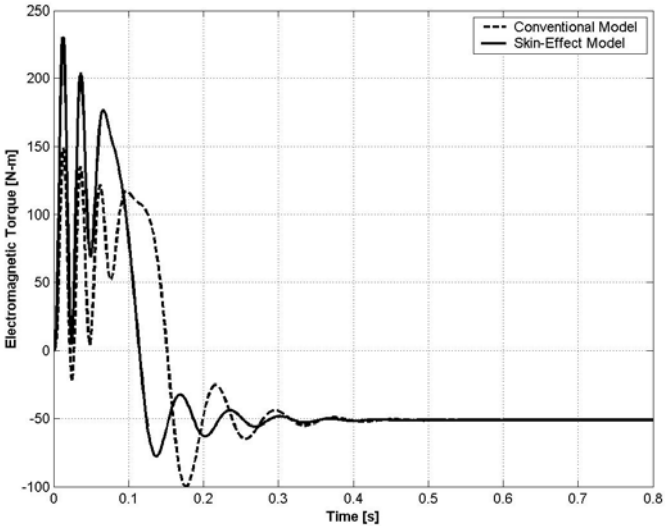

Figure 11: Electromagnetic Torque-Time Plot for the two Models.

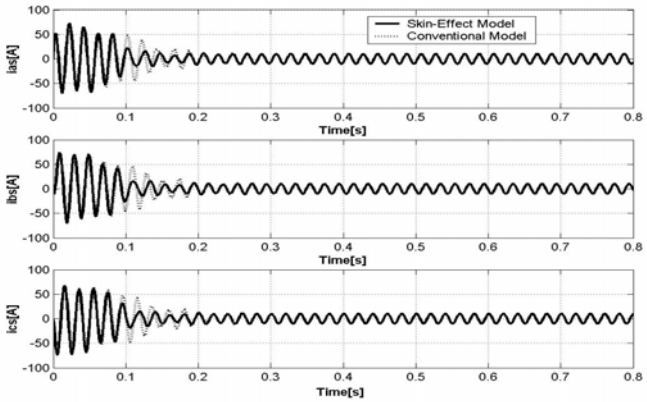

Figure 12: Stator Phase Currents-Time Plot for the two Models.

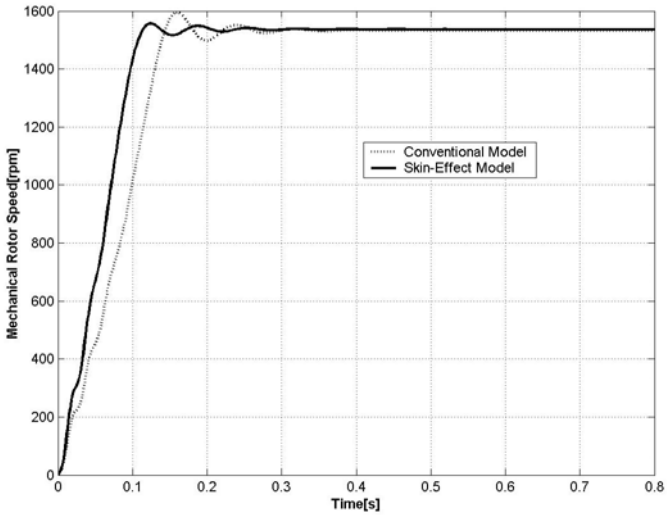

Figure 13: Mechanical Rotor Speed-Time Plot for the two Models.

The simulation results show that an accurate calculation of the inrush current and accelerating time cannot be realized by the conventional model, since the machine accelerates more rapidly than the model predicts. On the other hand, the skin-effect model presents better results. An improvement can still be achieved by the inclusion of saturation effect.

The technique developed in this paper should find widespread acceptance with those engineers engaged in the analysis and application of high horsepower industrial motor drives, and in area of renewable energy such as wind energy.

ACKNOWLEDGEMENT

The author wishes to express his thanks to DAAD for their financial support and to Prof. Dr.-Ing. B. Weidemann of the University of Kassel, Germany for his assistance and advice in producing this paper.

REFERENCES

[1.] Okoro, O.I. and T.C. Madueme. 2004. Solar Energy Investment in a Developing Economy. Renewable Energy. 29(9): 1599-1610.

[2.] Aliyu, U. O. and S.B. Elegba. 1990. Prospects for Small Hydropower Development for Rural Applications in Nigeria, Nigeria Journal of Renewable Energy, 1:74-86.

[3.] Oliver, G. et al. 1983. Evaluation of Phase–Commutated Converters for Slip-Power Control in Induction Drives. IEEE Trans. On Industry Appl. IA-19(1):105-112.

[4.] Oliver, G. and V.R. Stefanovic. 1982., Thyristor Current Source with an Improved Power Factor. IEEE Trans. Ind. Electronics. IE-29(4).

[5.] Krause, P.C. and C.H. Thomas. 1965. Simulation of Symmetrical Induction Machinery. Transactions IEEE. PAS-84(11) :1038-1053.

[6.] Vas, Peter. 1992. Electrical Machines and Drives: A Space-Vector Theory Approach. Clarendon Press: Oxford, UK.

[7.] Perdikaris, G.A. 1996. Computer Controlled Systems: Theory and Applications. Kluwer Academic Publishers: London, UK.

[8.] Okoro, O.I. 2002. Dynamic and Thermal Modeling of Induction Machine with Non-Linear Effects. Dissertation. University of Kassel, Germany.

[9.] Lipo, T.A. 1971. The Analysis of Induction Motors with Voltage Control by Symmetrically Triggered Thyristor. IEEE Transactions on Power Apparatus and Systems. PAS-90(2):515-525.

[10.] Levy, W. et al. 1990. Improved Models for the Simulation of Deep Bar Induction Motors, IEEE Transactions on Energy Conversion. 5(2):393-400.

[11.] Cornell, E.P. and T.A. Lipo. 1977. Modeling and Design of Controlled Current Induction Motor Drive Systems. IEEE Transactions on Industry Applications. IA-13(4):321-330.

[12.] Smith, A.C. 1995. A Transient Induction Motor Model Including Saturation and Deep Bar Effect. IEEE Transactions on Energy Conversion. 11(1):8-15.

[13.] Smith, J.R. 1990. Response Analysis of A.C. Electrical Machines: Computer Models and Simulation. John Willey and Sons: New-York, NY.

[14.] Alger, P.L. 1995. Induction Machines: Their Behaviour and Uses. Gordon and Breach Science Publishers: USA.

[15.] The Mathworks Inc. 1996. Using MATLAB, MATLAB: The Language of Technical Computing. The Mathworks Inc.: Natick, MA,

ABOUT THE AUTHOR

Dr.–Ing. O.I. Okoro holds a Ph.D. in Electrical Machines from the University of Kassel, Germany where he conducted his research under a DAAD Scholarship. He currently lectures in the Department of Electrical Engineering at the University of Nigeria, Nsukka. His research interests are in the areas of dynamic simulation and control of induction machines as well as in the thermal and dynamic analysis of AC machines. He is a member of the IEEE.

SUGGESTED CITATION

Okoro, O.I. 2004. Transient State Modeling of Asynchronous Generator with Skin Effect. *Pacific Journal of Science and Technology*. 5(2):63-71.